Dislocation Dynamics in Nanocrystalline Nickel

Z. W. Shan,[1] J. M. K Wiezorek,[2] E. A. Stach,[3] D. M. Follstaedt,[4] J. A. Knapp,[4] and S. X. Mao[1,*]

[1]*Department of Mechanical Engineering, University of Pittsburgh, Pittsburgh, Pennsylvania 15261, USA*
[2]*Department of Materials Science and Engineering, University of Pittsburgh, Pittsburgh, Pennsylvania 15261, USA*
[3]*School of Materials Engineering and Birck Nanotechnology Center, Purdue University, West Lafayette, Indiana 87185, USA*
[4]*Physical and Chemical Sciences Center, Sandia National Laboratories, Albuquerque, New Mexico 87185, USA*

(Received 28 March 2006; published 1 March 2007)

It is believed that the dynamics of dislocation processes during the deformation of nanocrystalline materials can only be visualized by computational simulations. Here we demonstrate that observations of dislocation processes during the deformation of nanocrystalline Ni with grain sizes as small as 10 nm can be achieved by using a combination of *in situ* tensile straining and high-resolution transmission electron microscopy. Trapped unit lattice dislocations are observed in strained grains as small as 5 nm, but subsequent relaxation leads to dislocation recombination.

DOI: 10.1103/PhysRevLett.98.095502 PACS numbers: 62.25.+g

Plastic deformation of crystalline materials is mainly carried by the generation, motion, interaction, storage, and annihilation of dislocations. These line defects connect two areas of a crystal that are sheared with respect to each other by an atomic translation called the Burgers vector. Atomistic simulations of 3D structures find that when grain size is reduced to deep nanoscale, i.e., with grain sizes typically less than 30 nm, only partial dislocations are emitted from grain boundaries of metals, which then glide through the grain and are absorbed at the opposite side of the grain [1–3]. Simulations also find that for very small grain sizes (approximately below 10 nm) plastic deformation is mostly carried by grain boundaries [2,4–6]. In order to investigate the deformation mechanisms of nanocrystalline materials, several *in situ* transmission electron microscopy (TEM) observations have also been performed [7–9]. Based on the contrast changes observed in the bright field TEM mode, it has been suggested [7,9] that dislocation mediated plasticity still plays a dominant role in the deformation of nanocrystalline Ni with a grain size less than 20 nm. However, no determination of the Burgers vectors was performed in these earlier experimental studies, although it is a critical issue for assessing the validity of the results from molecular dynamics simulations [1–3]. Additionally, knowledge of Burgers vector is needed as input into experiment-based models that are used to predict how dominant deformation mechanisms change when the grain size is below a critical value from being controlled by normal slip of unit dislocations to being controlled by partial dislocation activity, [10]. Also, the above observations apparently contradict previous postmortem TEM results [11], which failed to detect any evidence of dislocation activity in deformed nanocrystalline Ni with an average grain size of about 28 nm. To rationalize this discrepancy, Yamakov *et al.* [3] have suggested that extended dislocations can exist inside a nanoscale grain under very high stress and that the removal of this stabilizing stress would lead to the absorption of these partial dislocations by the grain boundary sources from which they originally nucleated. Unfortunately, traditional TEM sample preparation methods, such as mechanical thinning followed by ion thinning or twin-jet electropolishing inevitably result in relaxation of the stresses associated with the prior deformation. Hence, it is difficult to verify the intriguing predictions of these computational and theoretical studies. The current paucity of experimental data on the nature and the dynamics of dislocation activity in nanocrystalline metals critically limits the understanding of the deformation behavior and mechanical properties of these interesting materials.

The nanocrystalline Ni used in this study was synthesized by pulsed laser deposition with a nominal thickness of 150 nm [12]. TEM observations [Fig. 1(a)] indicate that the as-deposited Ni consists of roughly equiaxed grains with random orientations [electron diffraction pattern inset in Fig. 1(a)]. Statistically significant measurements using dark field TEM images [Fig. 1(b)] reveal a narrow, log-normal grain size distribution, ranging from several nm to 23 nm with an average grain size of about 10 nm [12]. High-resolution electron microscopy (HREM) shows that most of the grains are separated by high-angle grain boundaries. Furthermore, no additional grain boundary (GB) phases, porosity, or intergranular microcracks were detected in these high-quality samples.

In order to address the challenging problem of observing the microstructure of nanocrystalline Ni in a stressed state, a special sample design as used in Ref. [12] was adopted. The room temperature *in situ* tensile experiments were performed on a JEOL 3010 TEM with a single-tilt straining stage, which is operated at 300 kV with a point-to-point resolution of 2.1 Å. The loading process was controlled by applying pulses of displacement, and after each of the pulses the sample was held under stress for observation. After several initial incremental loading steps, a main crack as well as some branch cracks nucleated and propagated from the tip of the precrack. Areas in the plastically

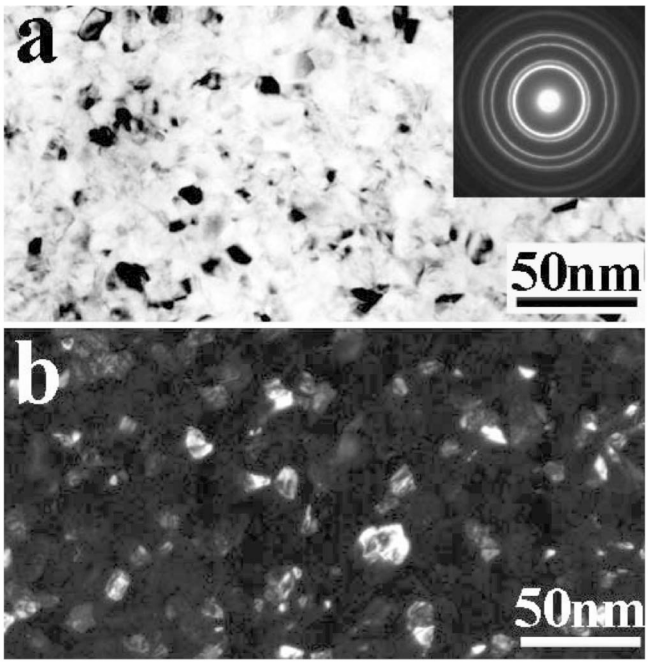

FIG. 1. TEM observations of the typical microstructure in the as-deposited nanocrystalline nickel films. The bright field TEM micrograph (a) and dark field TEM micrograph (b).

deformed zone ahead of these branch cracks were chosen for TEM observation because these areas experience significant local thinning during deformation, perhaps with just one grain through the thickness in some of these areas. Unlike the traditional TEM sample preparation techniques, where the thin areas are first prepared with ion thinning or electropolishing and then transferred to TEM for observation, the thin areas investigated in this work were freshly produced by the deformation in the high vacuum environment and therefore are less likely to be affected by contamination or other artifacts induced by sample preparation.

In order to detect trapped dislocations as well as to determine their Burgers vectors, HREM images of the strained samples were taken after they became sufficiently stable during the holding periods. Inspired by the results from molecular dynamics simulations [13] and the deformation twinning observed in aluminum, Chen *et al.* [10] proposed a dislocation model which predicted the existence of a critical grain size d_c, below which the deformation mechanism would change from one controlled by unit dislocations to one controlled by partial dislocations and twinning. According to this model, the critical grain size for Ni is about 11–22 nm [12]. Therefore, partial dislocation and/or twinning activities were expected to be prevalent in this experiment, where the average grain size in the sample was about 10 nm. However, neither partial dislocations nor deformation twinning have been identified thus far in the HREM images we have taken from these nanocrystalline Ni films after tensile loading. The lack of such evidence suggests that deformation twinning may not be generally present in nanometals, but rather is restricted to the special cases of high-pressure loading techniques, such as indentation, rolling, and high-pressure torsion [10,14–16].

However, trapped lattice dislocations were frequently detected in the deformed grains. An example HREM micrograph of two of these trapped dislocations is shown in Fig. 2(a). In the lower grain, a trapped dislocation in the vicinity of a GB can be clearly seen. The position of the dislocation is marked with a white $\perp$. Figure 2(b) depicts an inverse fast-fourier-filtered (IFFT) image of the region framed by the dark box in Fig. 2(a). The inset in Fig. 2(b) is the corresponding fast-Fourier-filtered (FFT) image, which confirms that the approximate electron beam direction is close to a $\langle 110 \rangle$ direction for this grain. Local Burgers

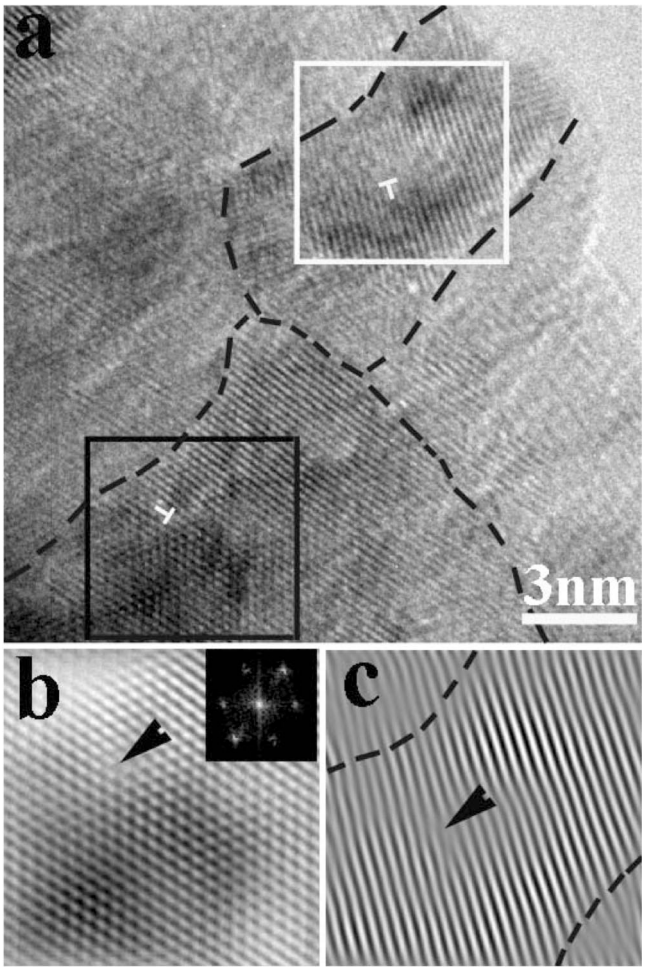

FIG. 2. (a) HREM micrograph of a thin area freshly formed by deformation. The white $\perp$'s and dark arrowheads indicate the position of a trapped unit lattice dislocation in the grain interior. Grain boundaries have been delineated by dark lines. (b) IFFT of the area framed with the dark box in (a). The Fourier-transformed image shown as an inset indicates that the electron beam is close to the 110 zone axis of the grain. (c) IFFT of the area framed with the white box in (a).

circuits were employed to determine the Burgers vectors of the dislocations in the HREM images. For the [110] zone axis image projection in Fig. 2(b), the measured displacement vector of the trapped dislocation is $\frac{a}{4}\langle 112\rangle$. Crystallographic analysis shows that this image is consistent with an actual Burgers vector of $b = \frac{a}{2}\langle 110\rangle$, a unit dislocation of the fcc lattice on a $\{111\}$ plane. A dislocation can also be seen in the middle of the upper grain in Fig. 2(a) with cross-sectional dimensions of approximately 5 nm $\times$ 10 nm. Figure 2(c) is an IFFT image of the area marked by the white square in Fig. 2(a), reconstructed using the spatial frequencies of the (200) planes.

As mentioned above, the grains in the areas studied were under stress during the displacement holding periods and dislocations were trapped in them. The sample is expected to relax to a lower energy state by structural changes. It is conceivable that this relaxation would lead to the rearrangement of these trapped dislocations. To study this process, a series of HREM images of a given stressed area that contained trapped dislocations was collected after a displacement pulse. Example HREM images extracted from such a dynamic sequence, which was taken over a relaxation period of 86 sec, are shown in Figs. 3(a) and 3(b). The strong ripple contrast in these figures may be taken as an indication that the area was experiencing substantial strain.

The locations of these trapped dislocations can be clearly identified from the IFFT images corresponding to Figs. 3(a) and 3(b), as shown in Fig. 3(c) and 3(d), respectively. A comparison of these images indicates that the dislocations marked with dark T's experienced no apparent displacement during the relaxation period, while those dislocations marked with white T's moved and rearranged. Using the dislocations marked with dark T's as reference, the upper two dislocations marked with white T's annihilated during the relaxation period. The two lower dislocations marked with white T's moved closer to each other during this time interval. The shrinkage and eventual annihilation of the trapped dislocation segments during this holding period in the nanocrystalline Ni confirm the prediction [3] that dislocations are most likely to be observed only when the grain is in a stressed state. However, it is inappropriate to equate the experimental observation here directly with behaviors observed during molecular dynamics simulations. Because of their subnanosecond time scale, molecular dynamics simulations can only capture the start of the deformation and thus exclude certain time-dependent processes. In contrast, due to the intrinsic stability requirements for imaging, the HREM observations only reveal the dislocation dynamics of the final state of the deformation. Efforts are still needed to uncover the entire process of dislocation dynamics in nanocrystalline materials.

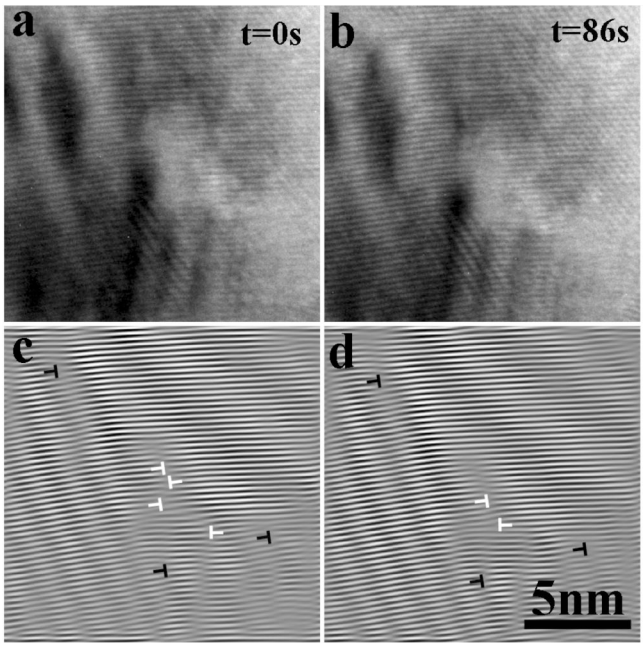

FIG. 3. Dynamical HREM observations of the microstructure evolution of a strained area during the stress relief. The positions of the dislocation cores have been indicated by T's. (a) $t = 0$, (b) $t = 86$ s, (c) IFFT of (a), and (d) IFFT of (b).

The relaxation process during the holding periods was very slow. At each time step of this process, the sample was in a quasistatic condition and the forces exerted on each dislocation were almost under equilibrium. Therefore, the dislocation activities in this relaxation process would be sluggish, somewhat akin to a creep process. The time interval between two states of the relaxation process illustrated by Figs. 3(a) and 3(b) was 86 sec. From the figures, we can see that distance between the two lower dislocations marked with white T's shortens only 1.5 nm.

In summary, we have demonstrated that observations of dislocation dynamics can be achieved by exploring a combination of *in situ* deformation and *in situ* HREM observation. The detection of trapped dislocations in grains as small as 5 by 10 nm confirmed that the as-deposited nanocrystalline Ni may exhibit very high yield strength. Deformation twinning may not be in general possible except for high-pressure loading techniques. Unlike the molecular dynamics simulations, which can only capture the very early part of the deformation of nanocrystalline materials, the results reported here only capture the final state of the deformation. Therefore, further efforts are necessary to reveal the entire process of nanocrystalline materials deformation.

This work was supported by the U.S. NSF Grant No. CMS-0140317 to the University of Pittsburgh. The work at NCEM was supported by the Director, Office of Science, Office of Basic Energy Sciences, Division of Materials Sciences and Engineering, of the U.S. Department of Energy under Contract No. DE-AC03-76SF00098. Work at SNL is supported by the Division of Materials Sciences and Engineering, Office of Basic

Energy Sciences, U.S. DOE. Sandia is a multiprogram laboratory operated by Sandia Corporation, a Lockheed Martin Company, for the U.S. Department of Energy's National Nuclear Security Administration under Contract No. DE-AC04-94-AL85000.

*Corresponding author.
Electronic address: smao@engr.pitt.edu

[1] H. Van Swygenhoven, P. M. Derlet, and A. Hasnaoui, Phys. Rev. B **66** 024101 (2002).
[2] H. Van Swygenhoven, Science **296**, 66 (2002).
[3] V. Yamakov, D. Wolf, M. Salazar, S. R. Phillpot, and H. Gleiter, Acta Mater. **49**, 2713 (2001).
[4] H. Van Swygenhoven, M. Spaczer, A. Caro, and D. Farkas, Phys. Rev. B **60**, 22 (1999).
[5] J. Schiotz, F. D. Di Tolla, and K. W. Jacobsen, Nature (London) **391**, 561 (1998).
[6] S. Yip, Nature (London) **391**, 532 (1998).
[7] R. C. Hugo, H. Kung, J. R. Weertman, R. Mitra, J. A. Knapp, and D. M. Follstaedt, Acta Mater. **51**, 1937 (2003).
[8] K. S. Kumar, S. Suresh, M. F. Chisholm, J. A. Horton, and P. Wang, Acta Mater. **51**, 387 (2003).
[9] R. Mitra, W. A. Chiou, and J. R. Weertman, J. Mater. Res. **19**, 1029 (2004).
[10] M. W. Chen, E. Ma, K. J. Hemker, H. W. Sheng, Y. M. Wang, and X. M. Cheng, Science **300**, 1275 (2003).
[11] M. Legros, B. R. Elliott, M. N. Rittner, J. R. Weertman, and K. J. Hemker, Philos. Mag. A **80**, 1017 (2000).
[12] Z. W. Shan, E. A. Stach, J. M. K. Wiezorek, J. A. Knapp, D. M. Follstaedt, and S. X. Mao, Science **305**, 654 (2004).
[13] V. Yamakov, D. Wolf, S. R. Phillpot, and H. Gleiter, Acta Mater. **50**, 5005 (2002).
[14] X. Z. Liao, F. Zhou, E. J. Lavernia, D. W. He, and Y. T. Zhu, Appl. Phys. Lett. **83**, 5062 (2003).
[15] X. Z. Liao, S. G. Srinivasan, Y. H. Zhao, M. I. Baskes, and Y. T. Zhu, Appl. Phys. Lett. **84**, 3564 (2004).
[16] A. Froseth, H. Van Swygenhoven, and P. M. Derlet, Acta Mater. **52**, 2259 (2004).